Coulomb-damped resonant generators using piezoelectric transduction

L. M. Miller, P. D. Mitcheson, E. Halvorsen, and P. K. Wright

Citation: Appl. Phys. Lett. **100**, 233901 (2012); doi: 10.1063/1.4726108
View online: http://dx.doi.org/10.1063/1.4726108
View Table of Contents: http://apl.aip.org/resource/1/APPLAB/v100/i23
Published by the American Institute of Physics.

Related Articles

Core loss behavior in high frequency high power transformers—II: Arbitrary excitation
J. Renewable Sustainable Energy 4, 033113 (2012)

Core loss behavior in high frequency high power transformers—I: Effect of core topology
J. Renewable Sustainable Energy 4, 033112 (2012)

Compact inductive energy storage pulse power system
Rev. Sci. Instrum. 83, 054703 (2012)

Uniform magnetic field distribution of a spatially structured resonant coil for wireless power transfer
Appl. Phys. Lett. 100, 214105 (2012)

The investigation of a compact auto-connected wire-wrapped pulsed transformer
Rev. Sci. Instrum. 83, 054702 (2012)

Additional information on Appl. Phys. Lett.

Journal Homepage: http://apl.aip.org/
Journal Information: http://apl.aip.org/about/about_the_journal
Top downloads: http://apl.aip.org/features/most_downloaded
Information for Authors: http://apl.aip.org/authors

ADVERTISEMENT

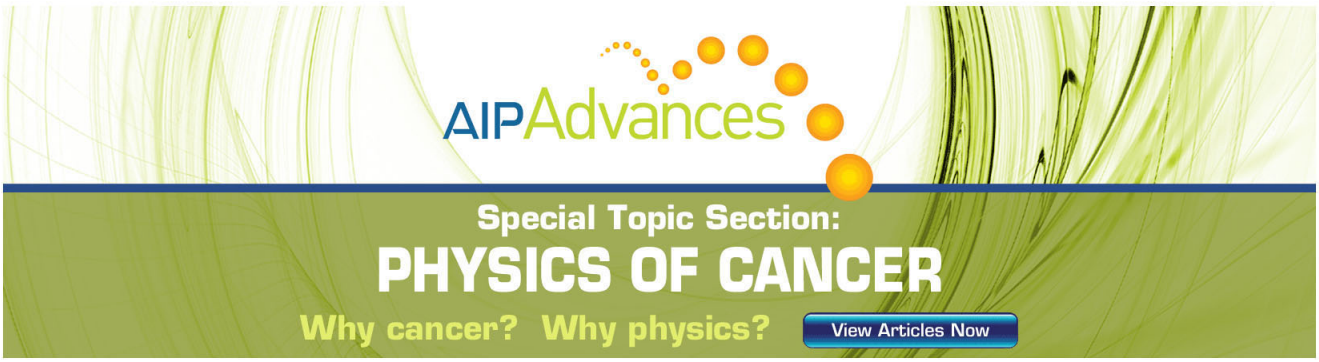

Downloaded 11 Jun 2012 to 128.248.155.225. Redistribution subject to AIP license or copyright; see http://apl.aip.org/about/rights_and_permissions

Coulomb-damped resonant generators using piezoelectric transduction

L. M. Miller,[1,a)] P. D. Mitcheson,[2,b)] E. Halvorsen,[3,c)] and P. K. Wright[4,d)]
[1]*Department of Mechanical Engineering, University of California, Berkeley, California 94720, USA*
[2]*Department of Electrical and Electronic Engineering, Imperial College, London SW7 2AZ, United Kingdom*
[3]*Department of Micro and Nano Systems Technology, Vestfold University College, Horten, Norway*
[4]*Department of Mechanical Engineering, University of California, Berkeley, California 94720, USA*

(Received 27 March 2012; accepted 10 May 2012; published online 5 June 2012)

Switching interface circuits employed with piezoelectric energy harvesters can increase the electrical damping considerably over that achievable with passive rectifiers. We show that a piezoelectric harvester coupled to certain types of switching circuits becomes a Coulomb-damped resonant generator. This allows analysis of such harvester systems within a well-known framework and, subject to practical constraints, allows the optimal electrical damping to be achieved. In the piezoelectric pre-biasing technique, the Coulomb damping is set by a pre-bias voltage whose optimal value is derived as a function of piezoelectric harvester parameters. © *2012 American Institute of Physics*. [http://dx.doi.org/10.1063/1.4726108]

Piezoelectric energy harvesting has attracted considerable interest and research efforts in the past decade due to the many applications of this technology in, for example, wireless sensor networks and biomedical devices.[1–3] In many applications, one of the challenges to obtaining successful piezoelectric energy harvesting devices is achieving an electrical damping high enough to obtain the desired levels of power output. This is especially true for MEMS-scale devices as the thin-film piezoelectric materials tend to exhibit lower electromechanical coupling coefficients than bulk piezoelectric materials.[4] Furthermore, MEMS devices tend to have a larger fraction of non-piezoelectric structural material in the cantilever which may further reduce the device electromechanical coupling factor.

Several interface circuit schemes to improve the achievable electrical damping for piezoelectric harvesters have been explored, such as synchronous electric charge extraction (SECE),[5] synchronous switched harvesting on inductor (SSHI),[6] and piezoelectric pre-biasing (PPB).[7] SSHI and PPB circuits have been shown to achieve power output approximately 8x and 16x, respectively, larger than that feasible with a simple optimal resistive load.[6,7] The advantage of the PPB circuit over the SSHI circuit is that the damping force can readily be set to the optimal damping as determined by the "mass in a box"[8] model. No circuit is capable of extracting more power than the limit of the "mass in a box" model, but the piezoelectric pre-biasing circuit is an efficient way of approaching that limit. The combined electromechanical analysis of piezoelectric harvesters connected to these switching circuits can be highly complex and this in turn makes the combined design a difficult task. Here a simple and intuitive approach to analyzing such systems is provided.

In this paper we describe how piezoelectric harvesters with a piezoelectric pre-biasing interface circuit can be analyzed in a framework already known to the energy harvesting community, that of the Coulomb-damped resonant generator (CDRG).[8,9] We then use this CDRG analysis to present the derivation of the Coulomb damping force in terms of the pre-bias voltage and other system parameters for a piezoelectric harvester connected to a PPB interface circuit. In this paper we consider interface circuits that modify the charge on the piezoelectric capacitor at the endpoints of travel of the cantilever (e.g., SSHI, SECE, and PPB circuits). We do not consider switched mode resistive emulation circuits, such as that presented by D'hulst *et al.*[10] as they do not provide the possibility of increasing the electrical damping force over that of a simple passive resistive load. We also assume the generator operates at resonance.

An example of a piezoelectric pre-biasing interface circuit is shown in Fig. 1. The detailed operation and experimental results verifying the functionality of that circuit are presented in Ref. 7. In the special case when the pre-bias voltage is zero, the PPB becomes a SECE configuration. Figure 2 shows how the voltage, charge, and force on the cantilever vary as the tip mass of the cantilever oscillates when the harvester is mechanically excited and connected to a PPB circuit. These diagrams show that switching occurs when the tip mass reaches its maximum and minimum positions and that charge is exchanged with the external circuit only at these instants.

With these waveforms in mind, we now examine the mechanical behavior of a piezoelectric harvester coupled to a PPB circuit. The constitutive equations of the piezoelectric *transducer* are, for our purposes, most conveniently written as

$$F = K_o z + \frac{\Gamma}{C_0} q, \tag{1}$$

$$V = \frac{\Gamma}{C_0} z + \frac{1}{C_0} q, \tag{2}$$

where F and V are force and voltage, K_o is open circuit stiffness of the beam, z is displacement of the proof mass attached to the end of the beam, q is charge on one of the piezoelectric transducer metal electrodes, and C_0 is the clamped

a)Electronic mail: lindsay@kingkong.me.berkeley.edu.
b)Electronic mail: paul.mitcheson@imperial.ac.uk.
c)Electronic mail: Einar.Halvorsen@hive.no.
d)Electronic mail: pwright@me.berkeley.edu.

 © 2012 American Institute of Physics

Downloaded 11 Jun 2012 to 128.248.155.225. Redistribution subject to AIP license or copyright; see http://apl.aip.org/about/rights_and_permissions

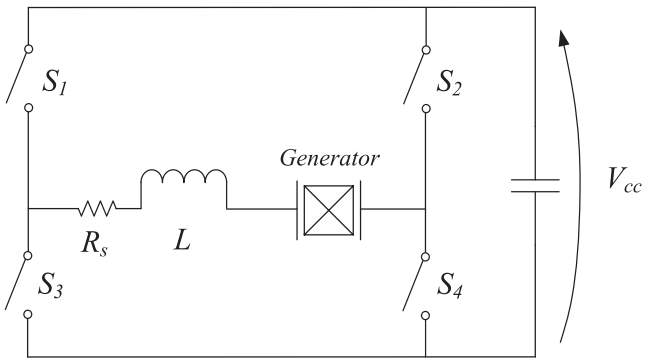

FIG. 1. Schematic of a simple PPB circuit configuration.

capacitance. Γ is the piezoelectric transduction factor.[11,12] For a cantilever device, it is proportional both to the piezoelectric material constant, e.g., d_{31} (or $e_{31,f}$ (Ref. 4)), and a factor that is dependent on the vibration mode in question.

The first term in Eq. (1) is the spring force (being proportional to proof mass displacement) and varies sinusoidally if the cantilever oscillates sinusoidally, while the second term is the force due to the charge present on the electrodes of the piezoelectric transducer due to action of the interface circuit. The value and variation over time of this second term depends on the behavior of the electrical circuit connected to the harvester, as well as the harvester's piezoelectric capacitance. The split between the two contributions to the force in Eq. (1) lets us view $\Gamma q/C_0$ as an electrical force and it is clear that if the charge is held constant for some time interval, then so is this electrical force. Hence, a circuit that remains disconnected from the piezoelectric electrodes on a half-cycle, such that the electrical force opposes the proof mass motion, implements a CDRG.

The sum of the two forces on the piezoelectric cantilever, F, is illustrated in the force diagram of Fig. 2, where the sinusoidal shape comes from the spring force and the offset that occurs at the peaks comes from the constant force due to charge. As can be seen in Fig. 2, the piezoelectric pre-biasing technique implements a perfect CDRG as the total force on the piezoelectric cantilever is the sum of a force which is proportional to cantilever position and a constant opposing force (between switching events) equivalent to a Coulomb damper.

Considering the alternative, but equivalent, formulation of the constitutive equation of the form $F = K_s z + \Gamma V$ where $K_s = K_o - \Gamma^2/C_0$ is the short circuit stiffness of the beam, we see that a similar argument can be made for circuits that give a piecewise constant voltage. This is the case for a perfect synchronous SSHI implementation, i.e., one with perfect charge inversion, as the piezoelectric voltage is clamped by the conduction of the diode rectifier during the entire half-cycle. However, for a realistic SSHI implementation with imperfect charge inversion, the voltage across the piezoelectric transducer is only clamped by the action of the diode rectifier as the cantilever approaches the extremes of its travel, as Fig. 3 illustrates. Therefore, a realistic SSHI implementation is not a perfect CDRG.

We now derive the system equations for a piezoelectric harvester connected to a PPB interface circuit in order to relate the piezoelectric parameters and pre-bias voltage to

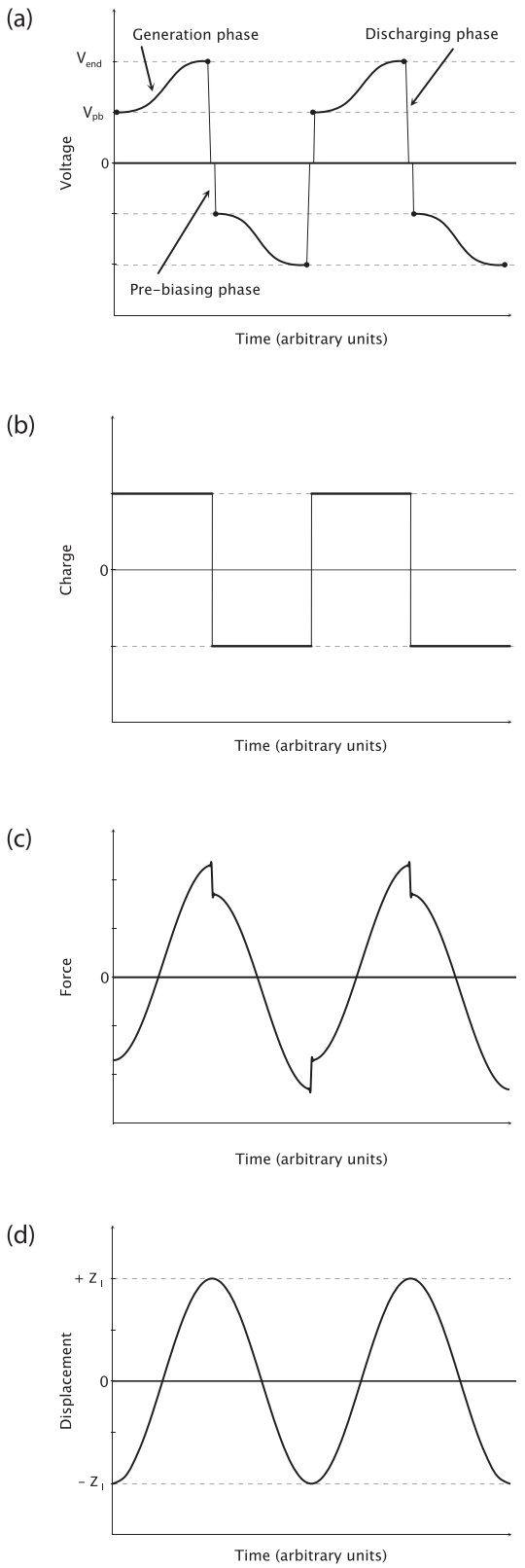

FIG. 2. Waveforms illustrating the voltage (a), charge (b), and force (c) on the piezoelectric harvester when connected with the PPB circuit and the corresponding harvester displacement (d).

the Coulomb damping force and system spring constant. An analysis has previously been presented in which the optimal Coulomb damping force has been calculated for a CDRG (Ref. 8) and, consequently, relating the Coulomb damping force to the piezoelectric properties will allow an optimal

Downloaded 11 Jun 2012 to 128.248.155.225. Redistribution subject to AIP license or copyright; see http://apl.aip.org/about/rights_and_permissions

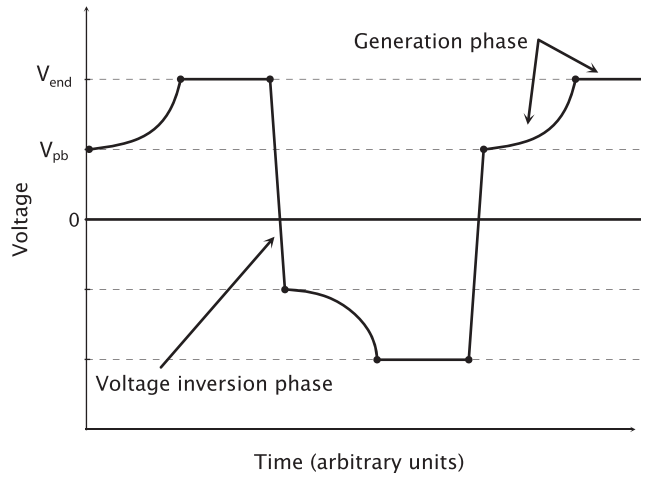

FIG. 3. Waveform illustrating the piezoelectric voltage with harvester connected to synchronous SSHI circuit. This is not a CDRG.

pre-bias voltage to be determined to maximize power generation. From Ref. 8, the optimal Coulomb damping force on a displacement-constrained CDRG harvester is

$$F_{\mathrm{opt_{CZ}}} = \frac{mY_0\omega^2\omega_c}{|U|}\sqrt{\frac{1}{(1-{\omega_c}^2)^2} - \frac{1}{{\omega_c}^4}\left(\frac{Z_l}{Y_0}\right)^2}, \quad (3)$$

where

$$U = \frac{\sin\left(\frac{\pi}{\omega_c}\right)}{1+\cos\left(\frac{\pi}{\omega_c}\right)} \quad (4)$$

and m is the proof mass, Y_0 is the input vibration amplitude, ω is the input excitation frequency, ω_c is the ratio of input excitation frequency to device resonance frequency, and Z_l is the maximum possible displacement due to packaging constraints. When $\omega_c = 1$, Eq. (3) simplifies to

$$F_{\mathrm{opt_{CZ}}} = \frac{\pi}{4}m\omega^2 Y_0 = \frac{\pi}{4}mA_{\mathrm{input}}. \quad (5)$$

Assuming that the cantilever is at its maximum positive displacement, Z_l, $F_{\mathrm{opt_{CZ}}}$ is equal to the Coulomb damping component of the force on the cantilever (second term in Eq. (1)). Solving this equality for q gives the relation,

$$q = -\frac{\pi}{4}mA_{\mathrm{input}}\frac{C_0}{\Gamma}. \quad (6)$$

The sign is negative because the Coulomb damping opposes the relative motion of the cantilever, acting against the spring restoring force. Substituting this expression for q into Eq. (2) and collecting terms gives the pre-bias voltage, V_{PB}, as

$$V_{\mathrm{PB}} = \left(-\frac{\pi}{4}mA_{\mathrm{input}} + \frac{\Gamma^2 Z_l}{C_0}\right)\frac{1}{\Gamma}, \quad (7)$$

which is the pre-bias voltage needed to obtain the optimal Coulomb damping force. When the cantilever is at the negative extreme of its travel, the polarity of the pre-bias voltage is reversed.

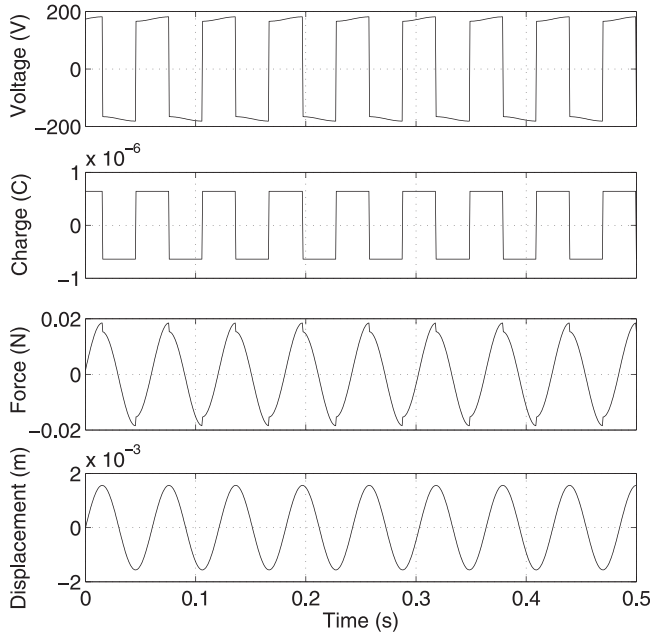

FIG. 4. Voltage, charge, force, and displacement on piezoelectric cantilever with PPB circuit calculated using CDRG framework.

It should be noted that, under certain operating conditions, the CDRG can exhibit start-stop motion which is undesirable due to difficulties in control.[8] However this phenomenon does not occur with optimal damping at resonance and so is not considered here.

Figure 4 shows results using this CDRG framework with realistic energy harvester parameters for an aluminum nitride MEMS scale harvester. The voltage, charge, and force on the piezoelectric cantilever corresponding with the position of the cantilever proof mass as it oscillates are shown. This illustrates the relative magnitudes of each variable for a realistic system.

This paper has discussed how a piezoelectric energy harvester can be made a perfect CDRG by connecting the mechanical system to a synchronously switched piezoelectric pre-biasing interface circuit. The differences in approximate and perfect CDRG behavior for piezoelectric harvesters with SSHI and piezoelectric pre-biasing circuits, respectively, were explained. Finally, equations were derived within the CDRG framework to find an expression for the pre-bias voltage which maximizes the power generation as a function of the input excitation and piezoelectric energy harvester parameters. These equations give the designer an easy way to calculate optimal pre-bias voltages for a piezoelectric transducer.

This work was supported by the Engineering and Physical Sciences Research Council (EPSRC) under Grant No. EP/G070180/1, "Next Generation Energy-Harvesting Electronics: Holistic Approach," the California Energy Commission Contract 500-01-43, the Demand Response project DR-03-01, and the Research Council of Norway Grant 191282 and SIU Contract No. NNA-2008/10004.

[1]S. Roundy and P. K. Wright, Smart Mater. Struct. **13**, 1131 (2004).
[2]M. A. Karami and D. J. Inman, Appl. Phys. Lett. **100**, 042901 (2012).

Downloaded 11 Jun 2012 to 128.248.155.225. Redistribution subject to AIP license or copyright; see http://apl.aip.org/about/rights_and_permissions

[3]M. Stewart, P. M. Weaver, and M. Cain, Appl. Phys. Lett. **100**, 073901 (2012).
[4]F. Calame and P. Muralt, Appl. Phys. Lett. **90**, 062907 (2007).
[5]E. Lefeuvre, A. Badel, C. Richard, and D. Guyomar, J. Intell. Mater. Syst. Struct. **16**, 865 (2005).
[6]D. Guyomar, A. Badel, E. Lefeuvre, and C. Richard, IEEE Trans. Ultrason., Ferroelectr., Freq. Control **52**, 584 (2005).
[7]J. Dicken, P. D. Mitcheson, I. Stoianov, and E. M. Yeatman, "Power-Extraction Circuits for Piezoelectric Energy Harvesters in Miniature and Low-Power Applications," IEEE Trans. Power Electron. Indust. Electron. (in press).
[8]P. D. Mitcheson, T. C. Green, E. M. Yeatman, and A. S. Holmes, J. Microelectromech. Syst. **13**, 429 (2004).
[9]D. Miki, Y. Suzuki, and N. Kasagi, in *Solid-State Sensors, Actuators and Microsystems Conference (Transducers)*, Denver, CO, 21–25 June 2009, pp. 636–639.
[10]R. D'hulst and J. Driesen, in *Power Electronics Specialists Conference*, Rhodes, Greece, 15–19 June 2008, pp. 2556–2562.
[11]H. A. C. Tilmans, J. Micromech. Microeng. **7**, 285 (1997).
[12]M. Renaud, K. Karakaya, T. Sterken, P. Fiorini, C. Van Hoof, and R. Puers, Sens. Actuators, A **145–146**, 380 (2008).

Downloaded 11 Jun 2012 to 128.248.155.225. Redistribution subject to AIP license or copyright; see http://apl.aip.org/about/rights_and_permissions